SPE 27888

Cost-Effective Monitoring of Injected Steam Migration Using Surface Deformation Analysis

M.S. Bruno, Chevron Petroleum Technology Co., and R.A. Bilak, Terralog Technologies Inc.

SPE Members

This paper was prepared for presentation at the Western Regional Meeting held in Long Beach, California, U.S.A., 23–25 March 1994.

ABSTRACT

Steam injection produces subsurface volume expansion due to increasing temperature and pressure within the injection interval. These subsurface deformations induce measurable surface displacements, including vertical and horizontal movements and tilt. Measurements and analysis of induced surface displacements often provide a cost effective method to monitor the extent and orientation of injected fluid migration patterns over large areas and to monitor subsurface zones of recompaction that may contribute to increased oil production during cyclic steam operations. This paper describes field measurement and numerical analysis techniques used to monitor steam injection processes and describes two case studies demonstrating the practical application of this technology.

INTRODUCTION

Design and management of an efficient multiwell steam operation requires anticipation and subsequent monitoring of both vertical and horizontal steam migration. While significant attention is often focused on establishing and maintaining vertical conformance and sweep, much less attention is focused on recognizing and accounting for non-uniform areal fluid migration. Many multiwell waterflood and EOR projects are installed with wells placed on symmetric patterns or evenly spaced lines based on the assumption that horizontal fluid flow will be completely symmetric. Unfortunately, areal fluid migration is often asymmetric. An analysis of 36 waterflood case histories by Heffer and Dowokpor[1] found a clear correlation between flow anisotropy and the direction of maximum horizontal stress in the reservoirs. Interestingly, the correlation was found to be equally as strong in fields identified as "unfractured" as in "fractured" reservoirs. These field results are consistent with laboratory experiments by Bruno et. al[2] describing stress-induced permeability anisotropy in weakly cemented sandstones. Failure to anticipate such anisotropy generally leads to premature breakthrough problems or poor areal sweep efficiency. On the other hand, recognition of asymmetric flow patterns early in a project will allow for optimizing well spacing and alignment, or improvements in subsequent infill well placement designs.

Most existing methods for mapping areal steam migration over large areas are relatively expensive. For example, installing 25 temperature observation wells to monitor a

one square kilometer [247 acres] area would cost about $750,000 to $1,000,000. Crosswell tomography or 3D seismic monitoring of the same area would be much more expensive. Surface deformation measurements and analyses provide a new and relatively inexpensive method to monitor areal steam migration. Although the information obtained is more qualitative than that available from temperature surveys, the technology can be applied at about one tenth the cost to cover large areas when other survey methods cannot be economically justified. Furthermore, surface deformation analysis can provide additional information on reservoir deformation processes, including shearing, volume dilation, and compaction, which are not readily available from other monitoring techniques. This paper presents a brief overview of surface deformation theory and field measurement techniques and describes two field studies demonstrating the application of this technology.

In one steam injection project surface displacements (vertical uplift) on the order of 5-10 mm [0.20-0.39 in] were measured during 4 precision level surveys over a 10 month period. Continuous readings of 7 near-surface tiltmeters were also recorded. The surface deformation pattern and analysis results demonstrated that steam migrated asymmetrically in a north-eastward direction from each of three injection wells. When steam injection was shifted among the wells, the position of maximum surface heave also shifted laterally, although the general pattern of asymmetric migration from each well remained consistent. Measured tilt orientations and reversals correlated well with downhole pressure cycles.

In a second project, steam was cyclically injected into 25 wells in alternating line patterns. Vertical displacements after injection cycles on the order 10 to 40 mm [0.39 to 1.57 in] and subsidence up to 14 mm [0.55 in] on subsequent flowback and production cycles were recorded. The measurements and analyses provided information on injected steam migration patterns as well as information regarding the location and timing of reservoir recompaction which was apparently affecting production. The surface deformation measurements and analyses have provided a cost-effective tool for evaluating steam processes at both of these EOR projects.

SURFACE DEFORMATION THEORY

Temperature and pressure induced volume expansion

Oil sand formation materials subjected to increased temperature and pressure will expand. The magnitude of volume expansion is dependent on the thermal expansion coefficients, compressibilities, and volume ratios of the oil, water, gas, and sand matrix. Under constant confining pressure, the total volume change ΔV of the oil sand materials subject to a change in temperature ΔT and fluid pore pressure ΔP is:

$$\Delta V = (\alpha_o V_o + \alpha_w V_w + \alpha_g V_g + \alpha_s V_s)\Delta T - (C_o V_o + C_w V_w + C_g V_g - C_s V_s)\Delta P \quad (1)$$

where α is the volumetric coefficient of thermal expansion, C is the compressibility, V is the volume, and the subscripts o, w, g, s refer to the oil, water, gas and sand matrix, respectively. Note that increased pore pressure compresses the fluids but expands the sand framework.

The expansion of the sand matrix, or bulk volume, is dependent on the amount of pore fluid drainage which occurs. The maximum expansion occurs under undrained conditions and the minimum expansion occurs under fully drained conditions. Laboratory tests[3,4] suggest that a 200°C change in temperature will induce volume expansion from 1% to 5% in some oil sands, depending on the saturation levels and drainage conditions. If the fluids are allowed to flow there will be little pressure increase due to thermal expansion, resulting in less volume expansion of the sand matrix.

Formation shear

In addition to volume expansion, temperature and pressure changes can induce shearing deformation within a reservoir. At least two types of formation shear mechanisms can occur: first, slip along sand/shale interfaces due to differential expansion of the materials; and second, shear dilation and sometimes planar slip within the oil sands due to a

pressure-induced decrease in effective vertical stress. Some volume expansion may also occur as the material shears and grains rearrange.

The first type of shear mechanism can be explained as follows. An oil sand zone may be bounded by two relatively impermeable zones, such as shale or mudstone layers. The perforation interval, higher oil saturation, and higher permeability all combine to cause the oil sand material to expand outwards to a greater extent than the bounding layers, resulting in shearing stresses and strains at the interfaces. Shear deformations are largest towards the periphery of the heated zone and smallest at the center. A well casing will therefore experience shear damage if the heated zone is asymmetric about the wellbore.

A second type of shear mechanism is illustrated in Figure 1. An increase in pore pressure, due to temperature and fluid injection, acts to reduce the effective vertical stress (overburden load minus pore pressure). Because the formation material is constrained from expanding laterally, the total horizontal stresses increase. The shear stress component which is related to the difference between the maximum horizontal stress and the vertical stress is increased while the mean normal stress is lowered, resulting in shearing failure and deformation. This type of formation shear can also be symmetric or asymmetric about the injection well, depending on the symmetry of the heated zone.

Surface deformations

Volume expansion and shear deformation in the subsurface will be transferred to surface deformations, with magnitudes determined by the material properties of the overburden. The shape of the surface deformation field is relatively insensitive to the subsurface zone dimensions in comparison to strike, dip, and depth to center. For many analyses the subsurface deformation zones may be assumed to be sufficiently well characterized by nearly planar discontinuities. For example, the surface deformation above a 10m thick zone experiencing 1% volume expansion is nearly identical to the surface deformation above a planar tension fracture located at the center of the 10m interval with a 10 cm opening displacement.

The surface displacements $SD(x,y)$ at any location above N subsurface deformation zones may be expressed as:

$$SD(x,y) = \sum_{n=1}^{N} F(xo_n, yo_n, zo_n, \delta_n, \beta_n, L_n, W_n, \Delta V, \Delta S) \quad (2)$$

where xo_n, yo_n, zo_n refer to the Cartesian coordinates of the origin of each deformation zone, and δ_n, β_n, L_n, and W_n refer to the dip, azimuth, length and width, respectively, of each deformation zone "n". ΔV and ΔS represent the subsurface volume expansion and shear displacement, respectively. F is the subsurface to surface transformation function. Details regarding this transfer function are provided by Davis[5] and Okada[6] for overburden materials assumed to be homogeneous and isotropic. Finite element models may be used to develop site specific transfer functions for heterogeneous and anisotropic overburden materials.

Surface displacements above a subsurface zone of volume expansion will be everywhere positive (heave) and generally symmetric above the center of expansion, as shown in Figure 2 for various dip angles. Surface displacements above a subsurface shear zone will be asymmetric above the shear center, with some negative displacements (subsidence) possible, as shown in Figure 3 for various dip angles.

Numerical inversion procedure

Equation (2) provides a numerical model for surface displacements expressed in terms of the location and geometry of subsurface zones of deformation. The inverse problem is to determine the subsurface deformation parameters from measured surface displacements. To accomplish this the following procedure may be applied:

1. A guess is made regarding the volume and geometry of deformation zones around each well.

2. Equation (2) is used to calculate theoretical surface displacements

produced by these assumed deformation zones.

3. The error between calculated displacements and field measured displacements is evaluated.

4. This error is minimized by adjusting the size and orientation of the deformation zones around the wells until the calculated and measured surface displacements agree to within the survey accuracy.

Subsurface deformation is assumed to occur due to both thermal expansion and pressure increase. Since the material properties of the overburden and the thermal and compressibility properties of the oil sand are not well known, it is not possible to use surface deformation magnitudes to determine subsurface temperature and pressure values quantitatively. It is possible, however, to use the shape of the surface deformation pattern to infer the areal pattern of the subsurface expansion zone qualitatively.

FIELD MEASUREMENT TECHNIQUES

Heave monument design and installation

Vertical surface deformations can be measured with high precision using specially designed heave monuments, such as the one shown in Figure 4. These are designed with a solid bottom anchor point which is driven into the formation material at a depth of about 7.6 m [25 feet]. A geotechnical drilling rig is used to auger a pilot hole and then drive the monuments into place. After the anchor is set, three prongs are driven and extended laterally into the formation. A 9.8 mm [0.25-inch] diameter pipe is used as the benchmark and extends from the lower anchor to the surface. This is protected by an outer 25 mm [1 in] casing which is disengaged from the anchor point after placement and lifted several inches, thus decoupling the anchor point from the upper 7 m [23 ft] of material. Any near surface deformation (which might result from temperature or saturation changes) should not produce movement in the anchor and attached benchmark.

Tiltmeter design and installation

Surface deformation may also be measured with borehole tiltmeters which produce DC signals proportional to tilt angle. These may be installed as shown in Figure 5 to help isolate the meters from surface vibrations, temperature, and saturation changes. Accuracy on the order of 1 microradian and range on the order of 1000 microradians is often sufficient for surface heave and subsidence monitoring. A temperature sensor is often included in the package. The 51 mm [2 in] diameter stainless steel cylindrical body is lowered into the inner casing and surrounded with dry sand. A cable transmitting three signals (two tilt vectors and one temperature) extends to the surface. The sand around the meter is tamped while monitoring the meter in order to zero the tilts. Accumulated data may be periodically downloaded manually at each borehole location. Alternatively, a surface or buried cable can transmit the signals from multiple tiltmeters to a central data acquisition system, which can be queried remotely by a modem and hardwired or cellular phone.

Surveying methods and error analysis

Surface displacements are measured periodically over an EOR project with first-order differential leveling techniques and computer assisted data processing. An external network of benchmarks is first installed outside the area of expected deformation. For example, for the first project described in this paper two clusters of external benchmarks were installed, with each containing three (3) ground rod benchmarks made of steel or aluminum rod driven by jackhammer until refusal. This configuration allowed establishment of local stability within each cluster (usually within 0.2 mm) and then global stability between the clusters.

Surface deformations measured with heave monuments are referenced to the average elevation of these external benchmark clusters. A preanalysis computation is performed assuming a free-network least-squares adjustment. None of the external reference points are considered as "fixed" in the adjustment computations. Through the use of statistical error analysis, careful observation techniques, and precise

equipment, vertical displacements may be measured to an accuracy of about 0.5 mm [0.02 in] at 95% confidence level.

STEAMDRIVE FIELD CASE STUDY

Site description

In this project steam was injected periodically into three wells, with bottomhole locations separated about 125 m (410 ft) apart along a line. The injection depth was about 250 m (820 ft) deep. Sixty eight (68) heave monuments were installed at the site covering an area roughly 600 m by 500 m (1970 ft x 1640 ft), as shown in Figure 6. Due to operational objectives and terrain conditions, a higher density of monuments was installed near the northernmost wells and a lower density around the southern section. Seven (7) tiltmeters were also installed surrounding the northernmost well. The injection interval was a relatively flat lying weakly consolidated sand formation, with some interbedded shale zones.

Injection and surface displacement summary

Comparison of the cumulative deformation and injection data provides convincing evidence that the measured surface deformations are directly related to subsurface steam migration patterns. This conclusion is further supported by the fact that monuments located at the periphery of the project (about 1/3 of the total) consistently exhibited no significant movement. During all stages of the project surface deformation was most extensive eastward from the injection wells. The eastward extending bulge tended to shift north-south as steam injection was shifted from well to well.

A summary of cumulative steam injection for each well, normalized with respect to the maximum volume injected, is presented in Figure 7. The sequence of cumulative surface deformations is summarized in Figure 8. For the period through February, 1992, more steam was injected into well W1 than either well W2 or W3. This was a period during which the largest deformation bulge occurred to the east of well W1, as shown in Figure 8a

From February through May, 1992, about three times more steam was injected into well W3 than into well W1, and about ten times more than into well W2. This is the period during which the center of the eastward trending surface bulge was farthest south (adjacent to well W3) as shown in Figure 8b.

Finally, from May through October, 1992, well W1 was shut in completely and roughly equal amounts of steam was injected first into well W3 and then into well W2 (about 25% less). This was the period of greatest injection into well W2 and coincided with the period of largest incremental deformation east of that well. The cumulative deformation bulge, shown in Figure 8c, shifted northward.

Subsurface deformation zone analysis

The numerical analysis techniques described above were used to estimate the progressive development of subsurface deformation zones induced by steam injection and to compare the field measurements with calculated displacements induced by the re-constructed deformation zones. The standard deviation of error between measured and calculated surface displacements normalized with respect to the average measured displacement for each survey period is provided in Table 1.

The maximum elevation change from January to February was 1.7 mm [0.067 in] and the average measured displacement of 66 points was only 0.39 mm [0.015 in], less than the survey sensitivity of about 0.8 mm [0.032 in]. The maximum elevation change from January to May was 5.0 mm [0.020 in] and the average measured displacement of 64 points was 1.84 mm [0.072 in]. Finally, the maximum elevation change from January to October was 7.2 mm [0.028 in] and the average measured displacement of 50 points was 3.36 mm [0.132 in]. For the initial period the standard deviation in error between the measured and calculated displacements is large compared to the average measurement, about 45%. By the final period, however, the standard error improves to 15% of the average measurement. A comparison of the measured and calculated surface displacements for the entire period is shown in Figures 9a and 9b, with the projection of the re-constructed subsurface deformation

zone superimposed on the calculated surface displacement pattern in Figure 9b.

The progressive patterns of subsurface deformation were generally consistent for each period. The zones extended continuously eastward from the injection wells and they expanded in size with time. At the end of the period from January through October, 1992, the relative size (area) and total deformation of the subsurface zones near each well were consistent with the relative amounts of steam injected into those wells. The largest zone and greatest deformation occurred east of well W3, into which the greatest amount of steam was injected. The second largest zone occurred east of well W1, into which the second largest amount of steam was injected. The smallest zone was located close to well W2.

Steamflood Case Study Discussion

Although the measured surface displacements over the first four surveys at this project site remained relatively small, they did provide an important qualitative indication of asymmetric steam migration towards the east. This eastward migration was confirmed in the area around well W1 with temperature observation wells. No temperature observation wells were available to the south of the project, but the consistent pattern of surface deformation as injection was shifted among the wells, combined with injection and production information, provided strong evidence that a similar flow pattern of eastward migration was occurring there as well.

While it is possible that lithology variations influenced horizontal steam migration at this site, in-situ stresses and shear dilation may have contributed to or even controlled the apparent permeability anisotropy. Stress-induced permeability anisotropy in high porosity and high permeability sands has been demonstrated in the laboratory by Bruno et. al[2]. An eastward trending steam path was consistent with the direction of maximum horizontal in-situ stress for the region and has been observed at other shallow steam projects[7]. These observations are consistent with an extensive review of waterflood projects by Heffer and Dowokpor[1] demonstrating a clear correlation between preferential fluid flow and the direction of maximum horizontal stress, even in "unfractured" reservoirs.

Tiltmeter observations

In addition to precision level surveys, surface deformations at this location were measured with an array of near-surface tiltmeters surrounding well W1 at distances of about 75 m [246 ft]. The purpose for monitoring tiltmeter data continuously is to compare results with survey measurements and to examine short term transient effects which may occur between the times at which precision level surveys are conducted. Although the original plan called for installation of 12 tiltmeters, very wet surface conditions resulted in poor coupling between the formation and the well casings leading to the decision to ultimately install only 7 meters. One of these meters subsequently went off scale early in the project and was not available for data analysis. The number of operating meters available was not sufficient for detailed surface deformation mapping or inversion calculations, but they did allow a qualitative examination of their potential application for future projects.

The cyclic variations in tilt correlate well with changes in steam injection rate and bottom hole pressure in well W1. Changes of slope in the tilt magnitudes and tilt angle polarity correspond to reversals in pressure buildup and decline. To illustrate this point, a comparison of the variation in the y-axis tilt magnitude for meters #4 and #6 with the change in bottom hole pressure at well W1 is presented in Figure 10. A comparison of the variation in x-axis tilt magnitude for meters #7 and #8 with the change in bottom hole pressure is presented in Figure 11.

Tilt angles calculated for alternating cycles of pressure buildup and decline demonstrated good repeatability. These are presented in Table 2. Tilt directions pointed away from the well during pressure increase cycles and towards the well during pressure decline cycles, indicating surface heave followed by subsidence. After the first cycle, the direction reversal is close to 180 degrees for all meters. Tilt angles calculated for the first

pressure decline period, however, differ from subsequent decline periods for some of the meters. It is possible that the volume of pressurized fluid was still too small to provide a consistent source signal during the first cycle. This volume increases with further injection so that for a given change in formation pressure, total volume expansion increases with time.

CYCLIC STEAM FIELD CASE STUDY

Site and process description

In this project twenty-five cyclic steam stimulation wells were completed within a heavy oil reservoir at a depth of 450m [1480 ft]. The producing formation was a 30m [98 ft] thick zone of 31% porosity oil sand. The wells were aligned in eight rows, as shown in Figure 12. Surface displacements were monitored with 186 benchmarks spaced on a regular grid over an area of about 1km by 1.36 km [3280 ft x 4460 ft]. The recovery strategy called for injection volumes of about $4000m^3$/well [25000 bbl/well] at typical rates of $160m^3$/day to $200m^3$/day [1000 bbl/day to 1260 bbl/day]. To maintain injectivity into the reservoir, injection pressures were established at close to overburden pressure, at or above fracture pressure. An overlapping row injection pattern was employed, whereby all wells in one initial row were steamed together and wells in an adjacent row began an injection cycle when 60% of the slug size had been injected into the initial row. A 4-6 day soak period followed the injection of steam, after which a production phase was implemented with a flow back and pumping period. The injection cycles started with well row #1 and followed through to well row #8.

Injection and deformation summary

Seven surface displacement surveys were completed and analyzed at this project. The displacement patterns for two north-south sections are presented in Figure 13, covering a period from July through September, 1991, during which rows #1, #2, and #3 were on production cycles, row #4 was shifted from production to injection, and rows #6, #7, and #8 were undergoing injection and soak cycles. As expected, the areas to the north (above injecting wells) are uplifted while the areas to the south (above producing wells) are subsided. The maximum uplift is about 30 mm (1.2 in) and the maximum subsidence is about 20 mm (0.79 in). The surface displacement patterns for two east-west sections during the same period are presented in Figure 14, showing the uplift along injection row #7 and subsidence along production row #3.

The measured displacements (points) compare well with calculated surface displacements (lines) determined from reconstructed reservoir deformations zones for the period, which are presented in Figure 15. In this figure well rows are labeled IC for injection cycle, FB for flow back, and PC for production cycles. Inversion of the surface data for the July to September period reveals that compaction is occurring along row #4 (darker shaded zones in Figure 15) while dilation is occurring along row #7. A sequence of reconstructed reservoir deformation patterns for two subsequent time periods is presented in Figures 16, and 17.

During the period from September to October, shown in Figure 16, rows #4 and #5 were undergoing production, row #6 was on flowback followed by lift production, row #7 was converted from injection to flowback, and row #8 was dominated by first cycle injection. In comparison with the previous period (Figure 15), reservoir compaction and dilation zones have each moved northward, consistent with the changing injection pattern. The large planes to the upper right in Figure 16 represent best-fit deformation from the injection activity, but are somewhat distorted due to limited survey coverage north of row #8. Finally, during the period from October to November shown in Figure 17, rows #7 and #8 were converted to flowback followed by lift production, and rows #1 and #2 were under injection. The previously dilating zones in the north recompacted and the southern section of the reservoir experienced new dilation.

Cyclic steam project discussion

During first cycle injection each deformation plane experiences shear slip, as much as 35

mm (1.4 in) average. The sense of motion is low angle thrust (6-15°), with the hanging wall moving up and away from the injection source. Slip is related to increase in horizontal total stress and decrease in vertical effective stress[8]. Shear displacements are largest during first injection cycles and become smaller during subsequent cycles, which are dominated by alternating dilation and compaction deformations.

The darker deformation planes shown in Figures 15, 16, and 17, are reconstructed recompaction zones, providing evidence of recoverable fabric dilation during injection. About 30% of the first cycle dilation was recovered during the first production cycle. This percentage rises in later cycles until subsidence roughly corresponds to uplift within each cycle, but with a permanent uplift component remaining from the initial irreversible dilation. Re-compaction occurs with almost no shear displacement; the compaction effect is purely volumetric due to the increasing effective vertical stress during production.

In this cyclic steam project re-compaction seemed to take place only during the initial stage of flowback and production. For example, consider compaction zones reconstructed during the second survey period shown in Figure 16. Although there is appreciable volume compaction in rows #5 and #6, very minimal volume compaction takes place in rows #3 and #4, despite continued fluid production. It was observed that wells in rows #3 and #4 during this period produced almost all water, whereas rows #5 and #6 undergoing compaction produced reasonable quantities of oil. These observations suggest that compaction drive was an important production mechanism during early portion of the production cycle, but that oil production could not be sustained. Apparently, continued production after the re-compaction phase only served to draw increasing amounts of mobile water.

COMPARATIVE COST SUMMARY

The cost to install and survey 100 monuments of the type used in these projects are summarized as follows:

Monument location survey	15,000
Monument materials	20,000
Monument installation	30,000
Total installation costs	$65,000
Periodic surveys (each)	$15,000

These are conservative estimates for normal terrain, but do not include any special costs that might be associated with clearing or grading rugged terrain. If the monuments are spaced about 100m apart, they would cover an area of about one square kilometer (about 250 acres).

To cover the same area with temperature observation wells, at a relatively sparse density of one every 10 acres, would require about 25 wells. Using slimhole completion techniques, these might be installed at a cost of $30,000 each, for a total cost of $750,000. This is more than ten times the costs required to cover the same area with 100 heave monuments. The costs for periodic temperature logging of 25 wells would be on the same order as the costs for periodic surveying of the 100 heave monuments.

DISCUSSION AND CONCLUSIONS

The numerical inversion process is often able to determine several possible solutions for subsurface deformation zone geometry which satisfy the criteria that the standard deviation of error between measured and calculated surface displacements be less than about 0.5 mm, the limit of accuracy for the field measurements. These solutions are usually consistent in general location and orientation, but vary in the details of geometric shape. The size and geometry of the calculated subsurface deformation zones should be considered as only qualitative indicators of heated fluid migration. Maximum deformation can be expected to occur at the outer boundary of the pressurized and heated zone where relatively undisturbed material is most affected.

Surface deformation analyses of the steamdrive and cyclic steam projects

described in this paper support the following conclusions:

1. Injected steam migration is often asymmetric around wells and patterns, generally in the direction of maximum horizontal in-situ stress.

2. Deformations induced by first cycle injection includes significant shear; later cycles are dominated by volume dilation.

3. Production cycles are dominated by volume compaction; little shear can be reconstructed.

4. Oil production seems directly related to recompaction magnitude and location.

5. Surface deformation analysis provides a cost effective tool for monitoring areal steam migration patterns and reservoir compaction drive mechanisms. Typical costs for large areas are far less than the costs required for monitoring with temperature observation wells.

In practice, temperature observation wells are used primarily to evaluate vertical sweep and conformance. Large arrays are rarely installed to capture areal migration patterns because of the relatively high costs required for extensive coverage. Although surface deformation analysis provides little information regarding vertical temperature variations, good qualitative information on areal expansion patterns and reservoir compaction zones may be obtained at low cost. The two monitoring techniques may be combined to provide an excellent tool for reservoir management in EOR processes.

NOMENCLATURE

α = Coefficient of thermal expansion
β = Deformation zone azimuth (degrees)
δ = Deformation zone dip angle (degrees)
C = Compressibility (MPa^{-1}) [psi^{-1}]
L = Deformation zone length (m) [ft]
P = Fluid pressure (MPa) [psi]
S = Shear displacement (m) [ft]
V = Volume (m^3) [ft^3]
W = Deformation zone width (m) [ft]
xo,yo,zo = Cartesian coordinates of deformation zones (m) [ft]

Subscripts
n = zone number
o = oil
w = water
g = gas
s = sand matrix

REFERENCES

1. K.F. Heffer and A.B. Dowokpor (1990) "Relationship between Azimuths of Flood Anisotropy and Local Earth Stresses in Oil Reservoirs", *North Sea Oil and Gas Reservoirs II*, The Norwegian Institute of Technology (Graham & Trotman, 1990).

2. M.S. Bruno, C.A. Bovberg and F.M. Nakagawa (1991), "Anisotropic Stress Influence on the Permeability of Weakly-cemented Sandstones", Proceedings of the 32nd U.S. Rock Mechanics Symposium, Norman, OK, July 10-12, pp.375-383.

3. M.B. Dusseault (1979). "Undrained Volume and Stress Change Behaviour of Unsaturated Very Dense Sands", Can. Geotech. J., Vol 16, pp. 627-640.

4. K.M. Kosar (1989), "Geotechnical Properties of Oil Sands and Related Strata", PhD Thesis, Dept. of Civil Eng., Univ. of Alberta, Edmonton, Canada.

5. P. Davis (1983), "Surface Deformation Associated with a Dipping Hydrofracture", J. Geoph. Res., Vol 88, pp. 5826-5834.

6. Y. Okada (1985), "Surface Deformation Due to Shear and Tensile Faults in a Half-Space," Bulletin of the Seism. Soc. Am., Vol. 75, No. 4, pp. 1135-1154.

7. P.R. Kry (1990), "Field Observations of Steam Distribution During Injection into the Cold Lake Reservoir," Rock at Great Depth, Maury & Fourmaintraux (eds.), (Balkema, Rotterdam) pp. 853-861.

8. M.B. Dusseault (1993) "Stress Changes in Thermal Operations", Proceedings 1993 International Thermal Operations Symposium, pp. 319-329, Paper SPE 25809.

Table 1. Average displacements and error analysis for each survey period

Survey Period	Average Displacement (no. pts)	Standard error dev Avg. Displ.
Jan-Feb, 1992	0.39 mm (66)	0.45
Jan-May, 1992	1.84 mm (64)	0.20
Jan-Oct, 1992	3.36 mm (50)	0.15

Table 2. Tilt directions during well W1 pressure cycles

	Pressure	Tilt Direction (deg. cw from plant north)			
Days	Behavior	Meter #4	Meter #6	Meter #7	Meter #8
15-20	increasing	88	75	346	61
20-25	decreasing	273	201	83	151
25-40	increasing	89	82	353	59
40-65	decreasing	271	271	166	218
65-78	increasing	91	88	339	62
78-83	decreasing	272	253	166	229

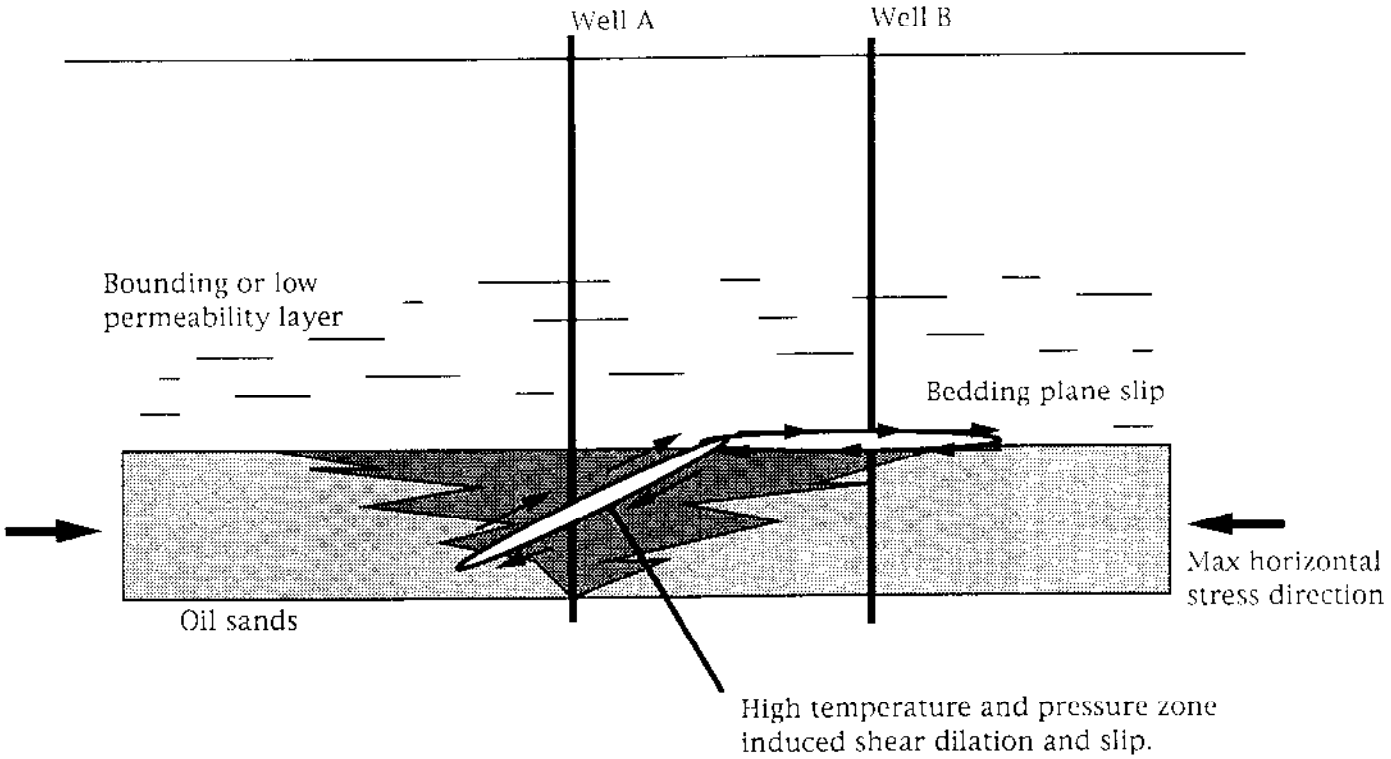

Figure 1. Increased temperature and pressure can sometimes relieve effective vertical stress enough to induce shearing in direction of maximum horizontal in-situ stress.

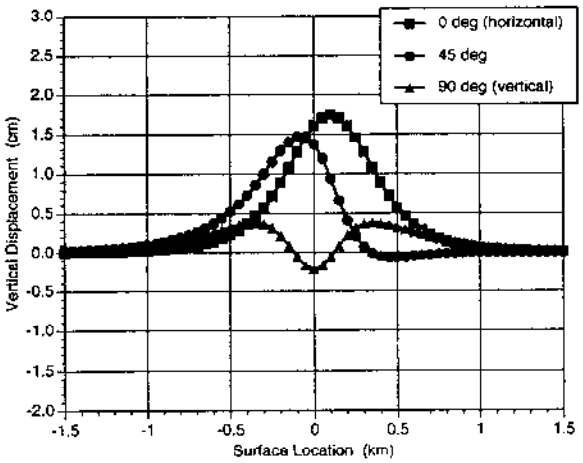

Figure 2. Surface displacements above a dilation zone (depth=500m; length=600m; width=200m; tensile displacement=10cm)

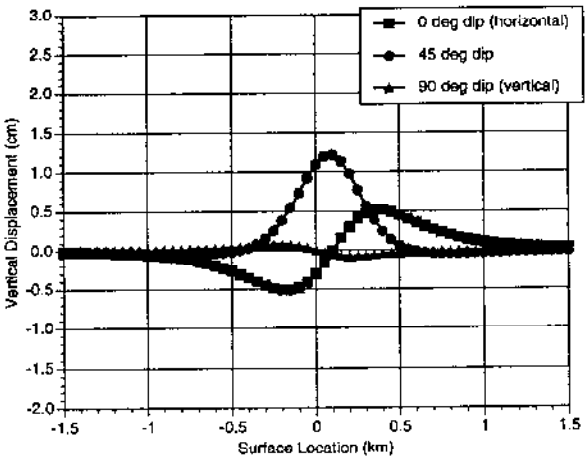

Figure 3. Surface displacements above a shear zone (depth=500m; length=600m; width=200m; tensile displacement=10cm)

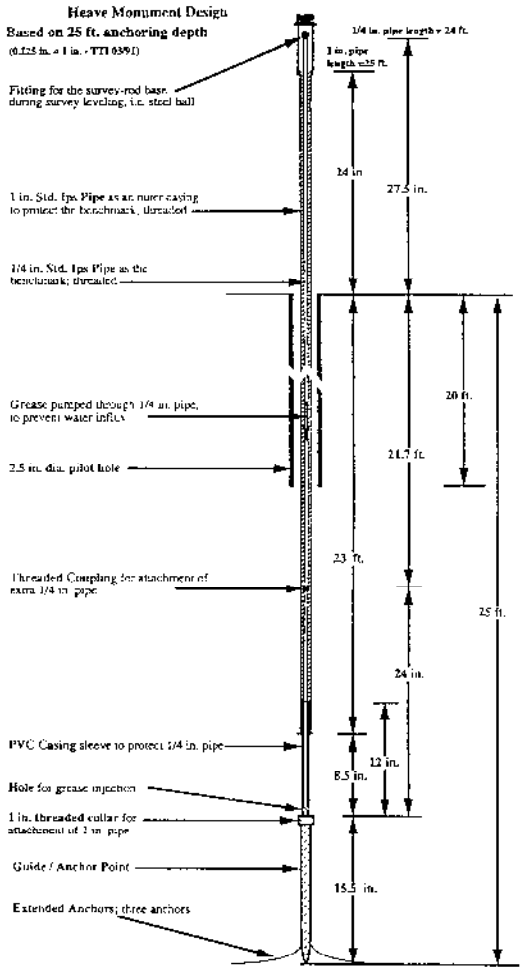

Figure 4. Typical heave monument design

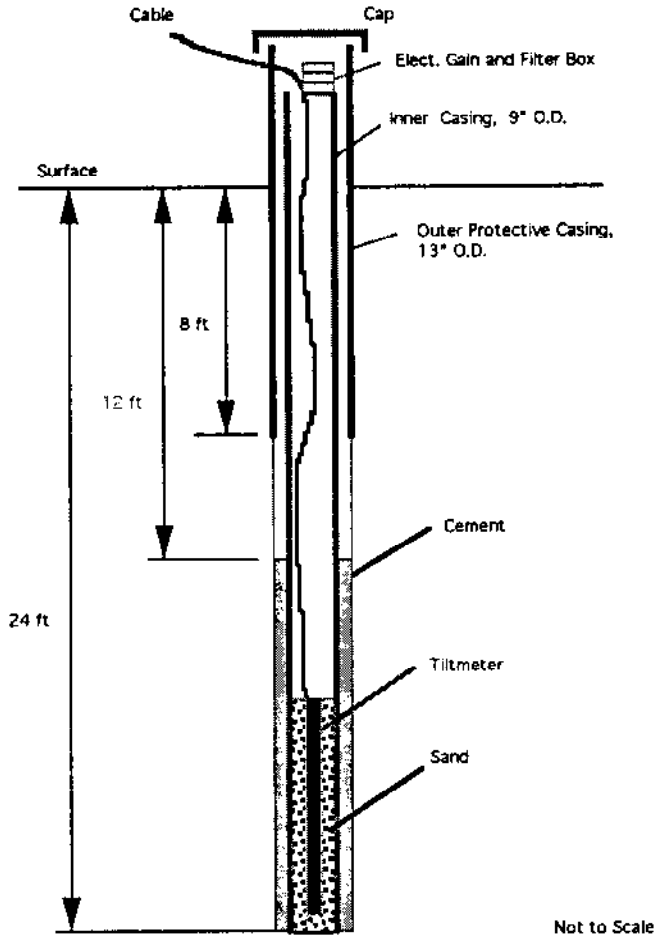

Figure 5. Typical tiltmeter installation

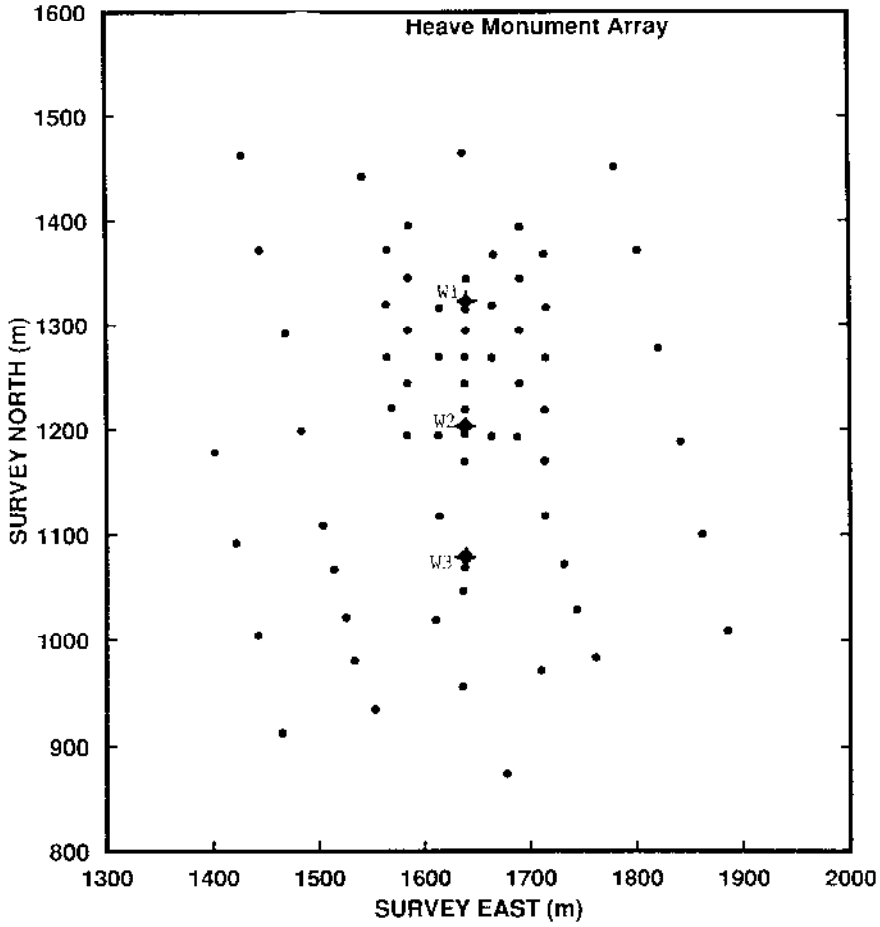

Figure 6. Steamdrive project site plan

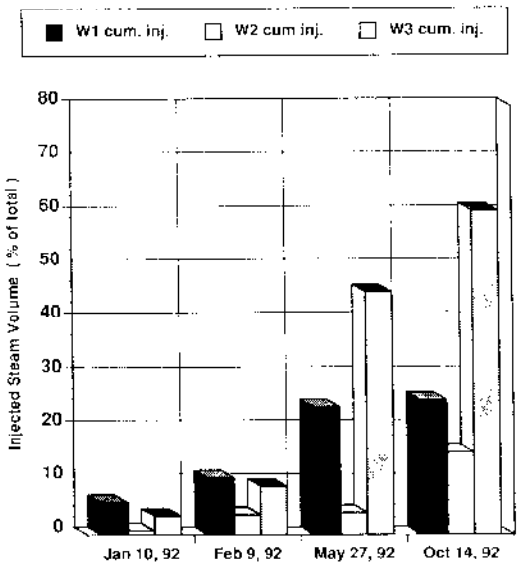

Figure 7. Steam injection summary for steamdrive project

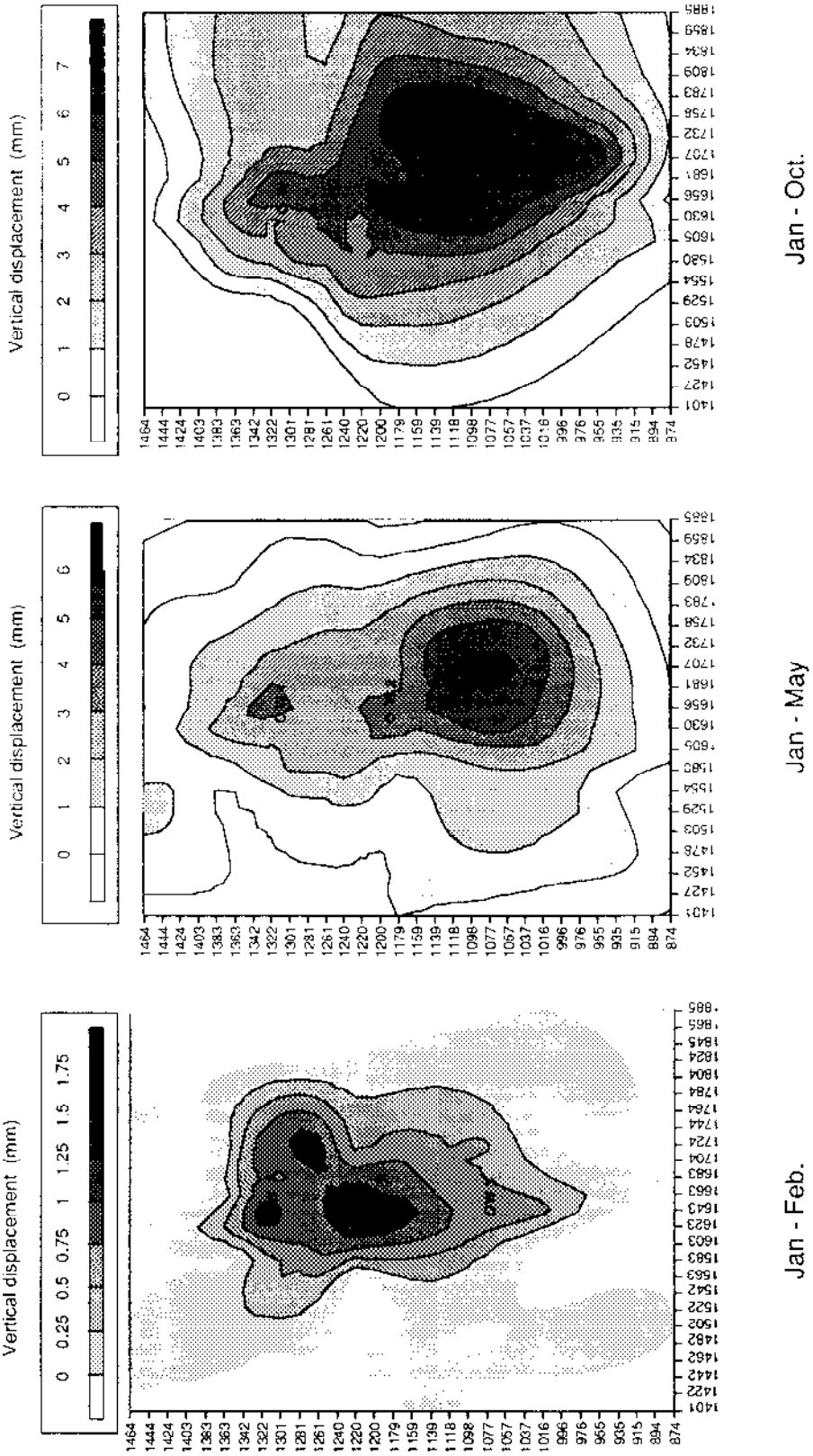

Figure 8. Cumulative surface displacements at steamdrive project from January through October, 1992.

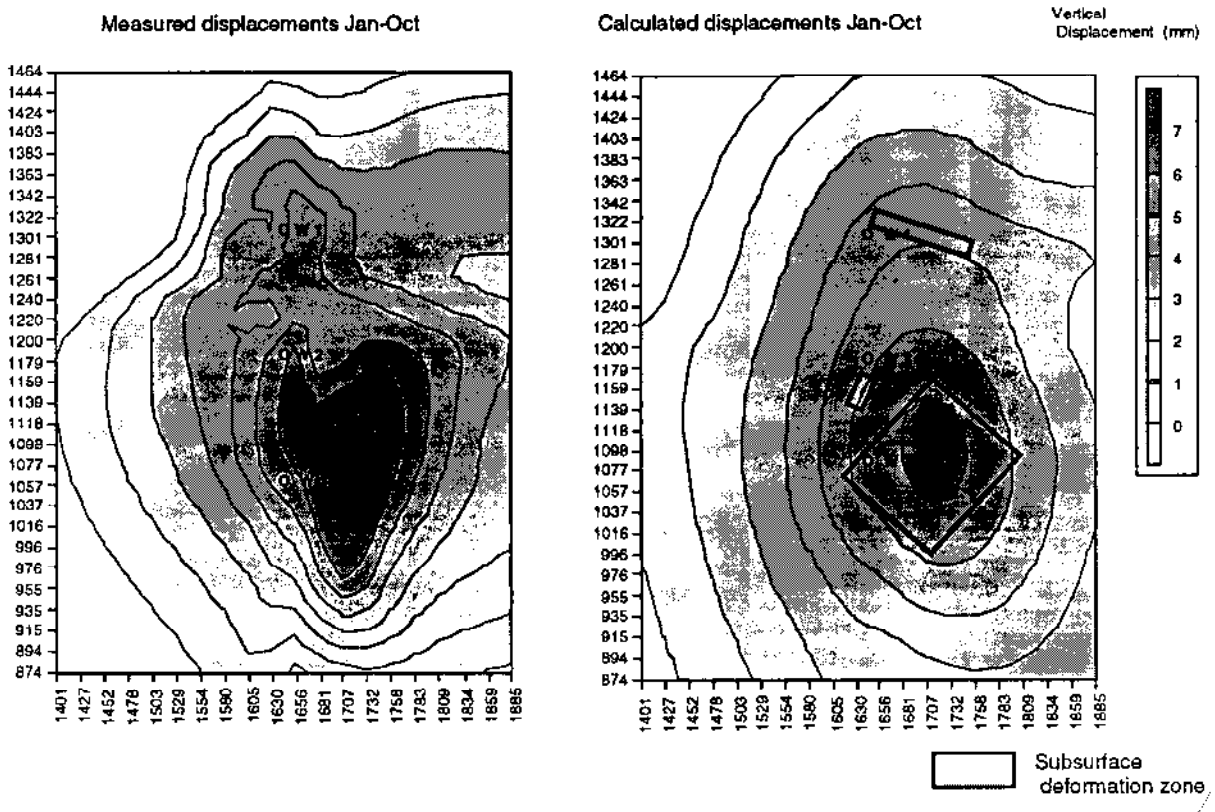

Figure 9. Comparison of cummulative and measured and calculated surface displacements at steamdrive project

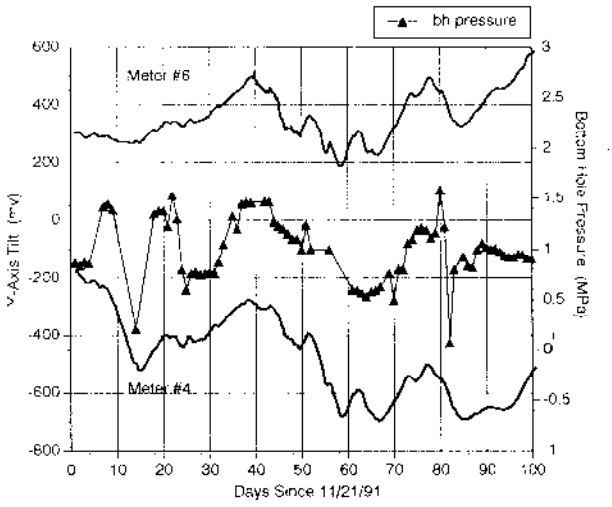

Figure 10. Y-axis tilt movement for meters #4 and #6 compared to bottomhole pressure in well W1 (scale = 0.2E-6 radians/mv)

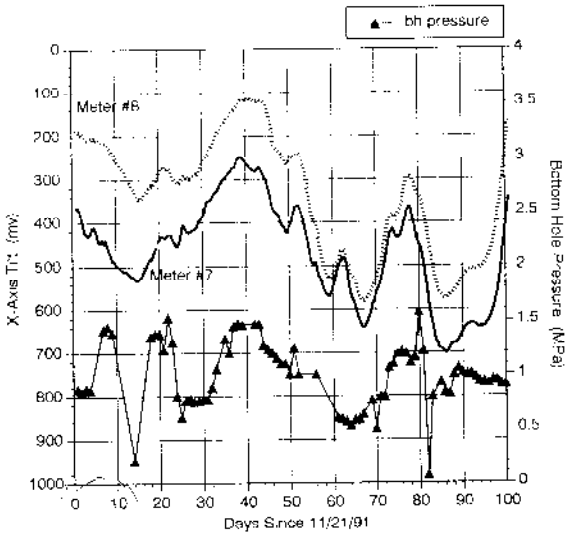

Figure 11. X-axis tilt movement for meters #7 and #8 compared to bottomhole pressure in well W1 (scale = 0.2E-6 radians/mv)

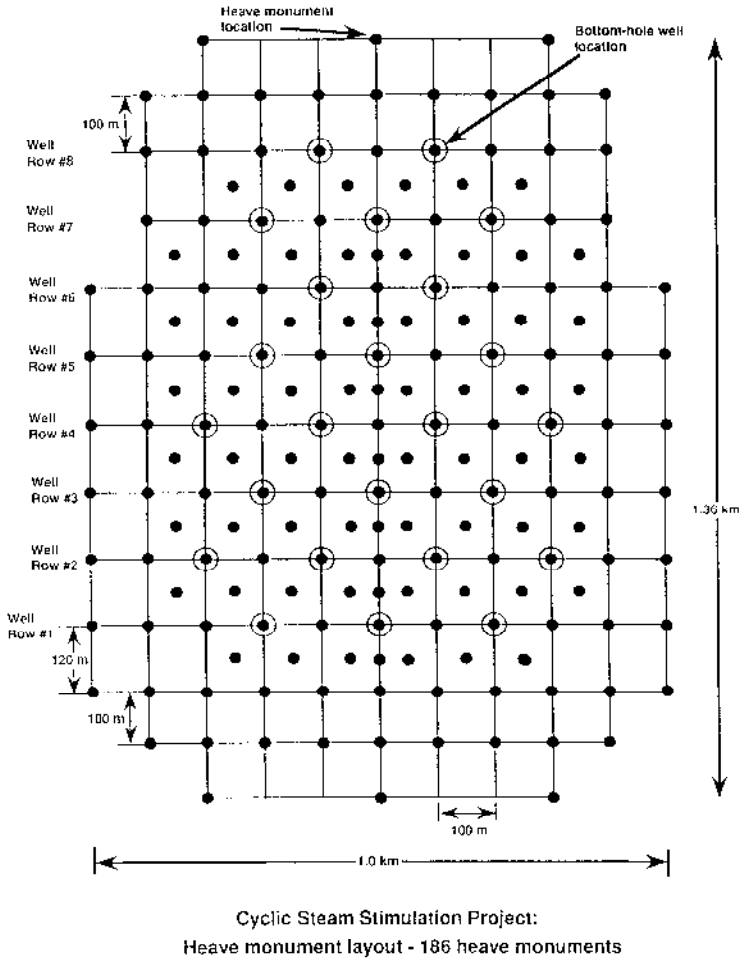

Figure 12. Cyclic steam project site plan

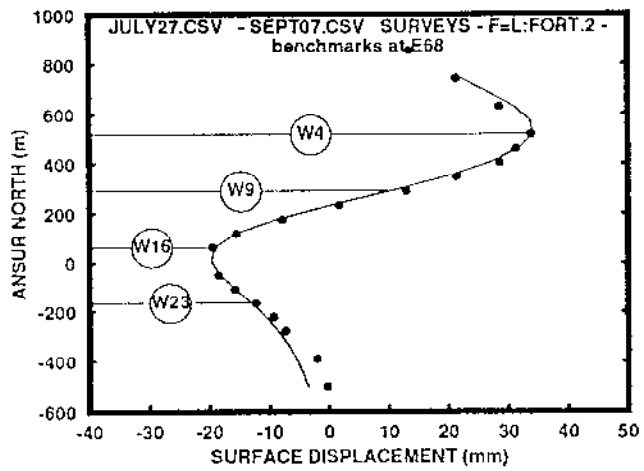

Figure 13. Comparison of measured and calculated displacements for N-S section through center of cyclic steam project for period from July to September.

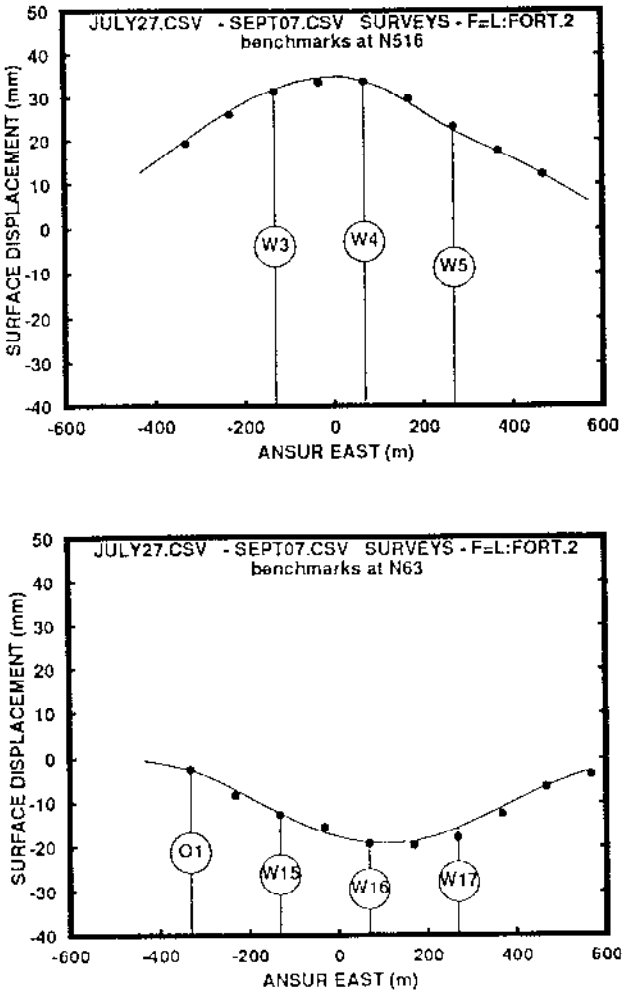

Figure 14. Comparison of measured and calculated displacements for E-W sections through row #7 (top) and row #3 (bottom) for period from July to September.

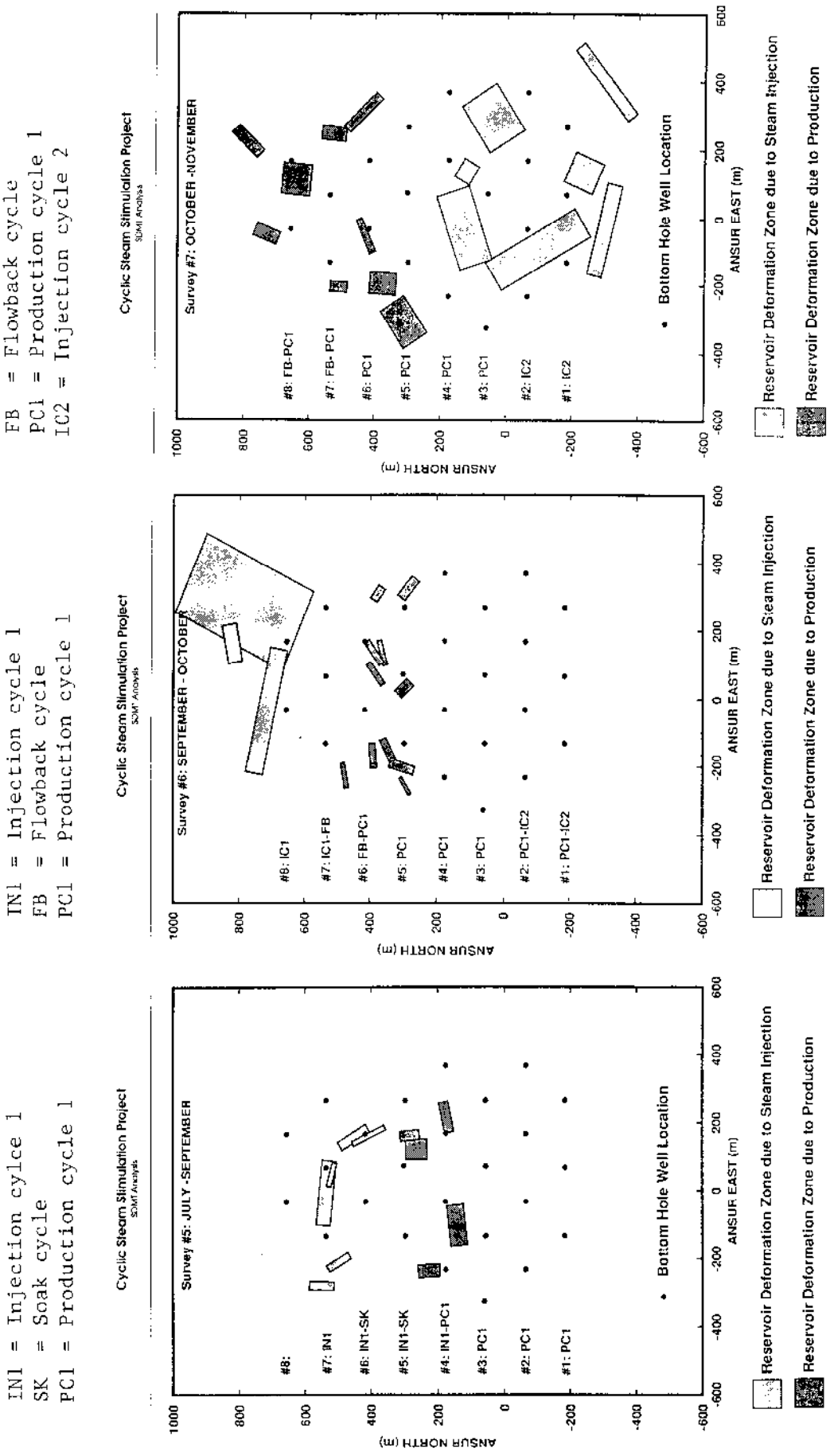

Figure 15.

Figure 16.

Figure 17.